Weak ferromagnetism induced by atomic disorder in Fe_2TiSn

A. Ślebarski,* M. B. Maple, E. J. Freeman, and C. Sirvent
Institute for Pure and Applied Physical Sciences, University of California, San Diego, La Jolla, California 92093-0360

D. Tworuszka, M. Orzechowska, and A. Wrona
Institute of Physics, University of Silesia, 40-007 Katowice, Poland

A. Jezierski
Institute of Molecular Physics, Polish Academy of Sciences, 60-179 Poznań, Poland

S. Chiuzbaian and M. Neumann
Universität Osnabrück, Fachbereich Physik, D-49069 Osnabrück, Germany

(Received 10 February 2000)

Electrical resistivity, magnetization, and specific-heat measurements on the Heusler-type alloy Fe_2TiSn reveal the occurrence of weak ferromagnetism below 240 K and heavy fermion behavior with a quasiparticle effective mass of ~ 40 times the free electron mass. *Ab initio* electronic structure calculations, which are in good agreement with measured x-ray photoemission valence-band spectra, yield a nonmagnetic ground state with a pseudogap located at the Fermi level. Atomic disorder inferred from Rietveld refinement of powder x-ray-diffraction data and its effect on the calculated electronic structure suggest that the weak ferromagnetism and the heavy fermion behavior may be induced by atomic disorder in Fe_2TiSn and other Heusler alloys as well.

Heusler-type alloys comprise a large class of ternary intermetallic compounds with the formula X_2YZ, where X and Y are two different transition metals and Z is a nonmagnetic metal or a nonmetallic element, which crystallize in a structure belonging to the space groups $L2_1$ or Cb_1.[1] Most of these compounds have a ferromagnetic ground state and are often found to exhibit some degree of atomic disorder. The origin of ferromagnetism and the effect of atomic disorder on the electronic properties of the Heusler alloys is not well understood and constitute a challenging problem. In this paper, we report electrical transport, thermal, magnetic, and x-ray photoemission (XPS) measurements on the Heusler-type alloy Fe_2TiSn which has not heretofore been investigated in detail[2] as well as *ab initio* electronic structure calculations using the localized muffin-tin orbital (LMTO) method. These measurements yield evidence of the formation of ferromagnetic correlations and heavy quasiparticles with an effective mass of ~ 40 times the free electron mass. The comparison of the XPS valence-band spectra with the band-structure calculations, with and without atomic disorder, suggests that the weakly ferromagnetic and heavy fermion behavior is induced by atomic disorder in Fe_2TiSn and, possibly, other Heusler alloys as well.

An Fe_2TiSn ingot was prepared by arc melting the constituent metals on a water-cooled copper hearth in a high-purity argon atmosphere. The sample was remelted several times to promote homogeneity, annealed at 800 °C for 1 week, and then quenched in water. The phase purity of the compound was ascertained by means of x-ray Debye-Scherrer diffraction with $Cu\,K_\alpha$ radiation using a Siemens D-5000 diffractometer. Magnetization measurements in the temperature range 2–300 K in magnetic fields up to 5 T were made using a superconducting quantum interference device magnetometer. A Faraday magnetometer was used to measure the susceptibility above room temperature. Electrical resistivity measurements were performed between 2 and 300 K using a standard four lead ac method. The XPS spectra were obtained with monochromatized $Al\,K_\alpha$ radiation at room temperature with a total energy resolution of about 0.4 eV using a PHI 5600ci ESCA spectrometer. The specific heat C was measured in the temperature range 0.6–70 K with a ^{3}He relaxation calorimeter using the heat-pulse technique. The electronic densities of states (DOS) were calculated using a spin-polarized self-consistent tight-binding linear muffin-tin orbital (LMTO) method,[3] within the framework of the local spin-density approximation.

A standard analysis of the peak positions in the powder x-ray-diffraction pattern for Fe_2TiSn showed that it crystallizes in an $L2_1$-type cubic structure with a lattice parameter of 0.6074 nm. However, a more detailed analysis of the x-ray-diffraction data in which the crystal structure of Fe_2TiSn was refined with the Rietveld method[4] revealed the presence of crystallographic disorder. The value of the R factor, $R_{wp}=4.9$, corresponds to the occupation of the Ti site by Fe in every fifth unit cell. Using Debye-Waller factors $B_i, i=$ Fe, Ti, or Sn, obtained from the fit, the Debye temperatures θ_{Di} at $T=300$ K were calculated from the relation $B_i(T)=(6h^2T/k_Bm_i\theta_{Di}^2)[\phi(\theta_{Di}/T)+\theta_{Di}/T]$, $\phi(\theta_{Di}/T)=\phi(x)=(1/x)\int_0^x(ydy/e^y-1)$,[5] where m_i is the atomic mass. The value of the Debye temperature obtained for the Fe_2TiSn sample, $\theta_D=\frac{1}{4}\Sigma\theta_{Di}$, is 415 K.

Displayed in Fig. 1 is a plot of the lattice parameters a determined from x-ray-diffraction measurements at various temperatures T. Also shown in the figure, for comparison, is the expected behavior of $a(T)$, calculated from the Debye lattice vibration model. The temperature dependence of a

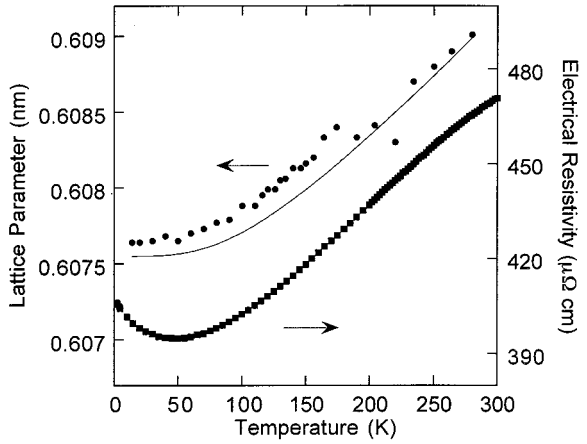

FIG. 1. Lattice parameter a and electrical resistivity ρ vs temperature for Fe_2TiSn. The solid curve is the experimental behavior of the lattice parameter of Fe_2TiSn, calculated on the basis of the Debye lattice vibration model.

was derived from the coefficient of linear thermal expansion α_L which can be expressed as $\alpha_L = K_L \gamma_L C_L/3V$, where C_L is the specific heat, K_L is the isothermal compressibility, and γ_L is the Grüneissen constant. It was assumed that K_L and γ_L are temperature independent and $K_L \gamma_L/3V = \alpha_{\exp}/C_L = \mathcal{A}$ at room temperature, while $\alpha_L(T) = \mathcal{A} C_L(T)$ below room temperature, where $C_L(T)$ was calculated from the Debye model using the value $\theta_D = 415$ K determined from the Rietveld refinement of the x-ray-diffraction pattern for Fe_2TiSn. At 240 K, there is an abrupt drop in the experimental a vs T plot relative to the calculated $a(T)$ curve. As discussed in the following, this drop in $a(T)$ coincides with some rather dramatic features in $\chi(T)$.

Shown in Fig. 2 are magnetic susceptibility χ data, plotted as χ vs T and χ^{-1} vs T, between 2 and 450 K. The $\chi(T)$ [and $\chi^{-1}(T)$] data exhibit thermal hysteresis in the vicinity of 250 K. The inverse magnetic susceptibility χ^{-1} follows a

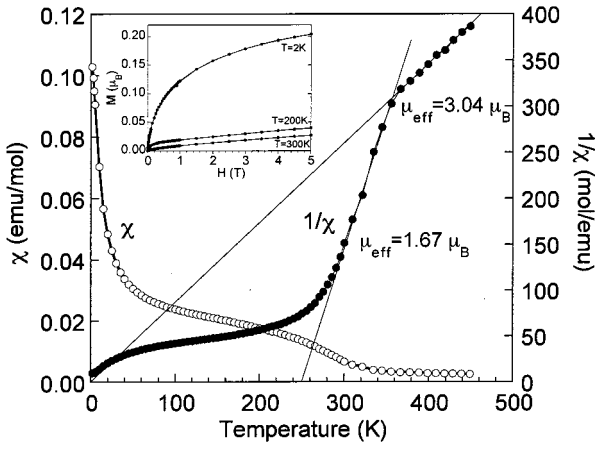

FIG. 2. Magnetic susceptibility χ and the inverse susceptibility χ^{-1} vs temperature for Fe_2TiSn. The applied magnetic field was 5 kOe. The solid lines represent linear extrapolations of χ^{-1} vs T plots. For $T > 350$ K, $\mu_{eff} = 3.04\,\mu_B$ and $\theta = 0$, while for $280 < T < 350$ K, $\mu_{eff} = 1.67 \mu_B$, and $\theta = 250$ K. Inset; magnetization vs magnetic field at constant temperature.

Curie law above 350 K, but deviates markedly from the Curie law below 350 K, signaling the onset of the weak ferromagnetism. A least-squares fit of the $\chi(T)$ data from 250 to 350 K to a Curie-Weiss law $\chi(T) = C/(T-\theta) + \chi_0$ where $C = N_A \mu_{eff}^2/(3k_B)$, N_A is Avogadro's number, μ_{eff} is the effective moment, μ_B is the Bohr magneton, and θ is the Curie-Weiss temperature, yields $\mu_{eff} \cong 1.6\mu_B$, $\theta \cong 250$ K, and $\chi_0 = 1.1 \times 10^{-3}$ emu/mol. In contrast, a least-squares fit of the data from 350 to 450 K to a Curie law $\chi(T) = C/T$ gives $\mu_{eff} \sim 3.1\mu_B$, close to the effective moment of pure iron. For other specimens prepared in nearly the same way, θ and μ_{eff} obtained from the Curie-Weiss fits differ by as much as 15% from the values found from the data in Fig. 2. We attribute the change in the χ^{-1} vs T plot that occurs at ~ 350 K to a diffusion process that results in a more highly ordered sample above ~ 350 K that exhibits paramagnetic behavior (i.e., $\theta \cong 0$ K). We are aware of other examples among Heusler-type alloys where annealing does not produce crystallographic ordering, while cycling the temperature results in a more ordered material above ~ 350 K, reflected in, for example, resistivity measurements.[6] Magnetization curves, measured up to 5 T at 2, 200, and 300 K, shown in the inset of Fig. 2, reveal a small amount of hysteresis at 2 and 200 K, providing additional evidence for local moment ferromagnetism in Fe_2TiSn. The saturation magnetic moment μ_s, obtained from an extrapolation of an M vs $1/H$ plot to $1/H \to 0$, is $0.26\mu_B$.

In Fig. 3, we present numerical calculations of the DOS of Fe_2TiSn for different occupations of the crystallographic positions in the unit cell: (a) Fe atoms in $8c$ sites, Ti atoms in $4b$ sites, and Sn atoms in $4a$ sites; (b) one Fe atom in a Ti $4b$ site; and (c) two Fe atoms in Ti $4b$ sites. For the ordered crystal [case (a)], the LMTO calculations yield a nonmagnetic ground state and a pseudogap at the Fermi level ϵ_F. The local disorder leads to ferromagnetism and a magnetic moment per formula unit of $1.46\mu_B$ in case (b) and $3.18\mu_B$ in case (c). As mentioned above, the Rietveld fit to the x-ray-diffraction data of Fe_2TiSn yields a supercell with a lattice parameter $5 \times a$ with one Fe atom occupying a Ti position in every supercell. On the basis of LMTO calculations, we estimate the magnetic moment $\mu = 0.29\mu_B$ per formula unit, in a good agreement with the observed value $\mu_s = 0.26\mu_B$. This also provides a possible explanation for the $\chi(T)$ behavior in Fig. 2. Every fifth disordered unit cell can be regarded as a ''magnetic impurity''; the interaction between these ''magnetic impurities'' via the long-range Ruderman-Kittel-Kasuya-Yosida mechanism may explain the weak ferromagnetism observed in the Curie-Weiss behavior between 0 and 350 K.

Another possible source of the weak ferromagnetism in Fe_2TiSn is a volume effect. Shown in Fig. 4 is a plot of the calculated total energy, relative to its minimum value, and magnetic moment μ vs the Wigner-Seitz radius r_{WS} (or equivalently, the Wigner-Seitz volume, $V_{WS} = 4\pi/3 r_{WS}^3$). According to the calculated μ values shown in Fig. 4, Fe_2TiSn exhibits magnetic behavior ($\mu > 0$) above the critical value $r_{WS} = 11.7$. The critical value of r_{WS} is, however, significantly larger than the value at which the onset of ferromagnetism is observed. Thus we conclude that the influ-

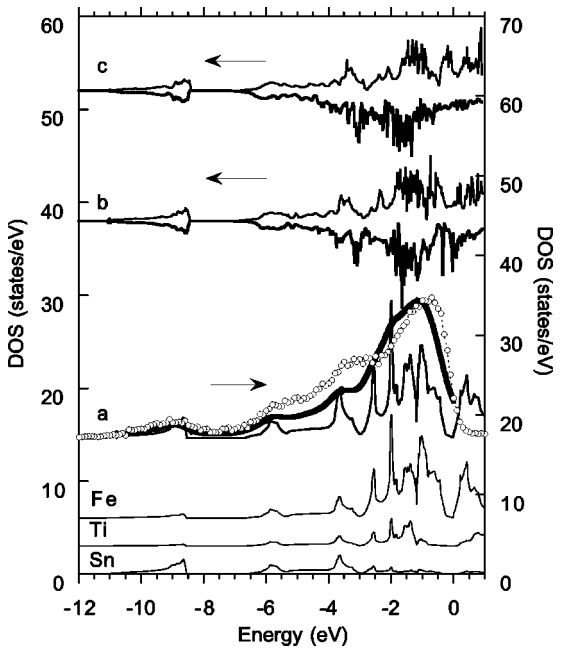

FIG. 3. Numerical calculations of the DOS of Fe_2TiSn (space group: $Fm3m$) for both spin directions, taking into consideration the substitution of Ti and Fe atoms for each other. The chemical formula is $(Fe_{2-x}Ti_x)(Ti_{1-x}Fe_x)$ Sn with $x=0(a)$, $x=0.25(b)$, and $x=0.5(c)$. In $(a)(x=0)$, the total DOS calculated for the paramagnetic Fe_2TiSn (thin curve), convoluted by Lorentzians of half-width 0.4 eV, taking into account proper cross sections for bands with different l symmetry (thick curve), is compared to the measured XPS valence-band data corrected for background (open points). The partial DOS curves for Fe, Ti, and Sn are plotted below.

ence of volume on the formation of the magnetic ground state in Fe_2TiSn can be disregarded.

Turning now to the gap at ϵ_F which is apparent in the calculated DOS at $T=0$ (Fig. 3), we find that this pseudogap is strongly reduced by the atomic disorder. A convenient way to observe the gap is to measure the temperature dependence of the electrical resistivity ρ. Shown in Fig. 1 are ρ vs

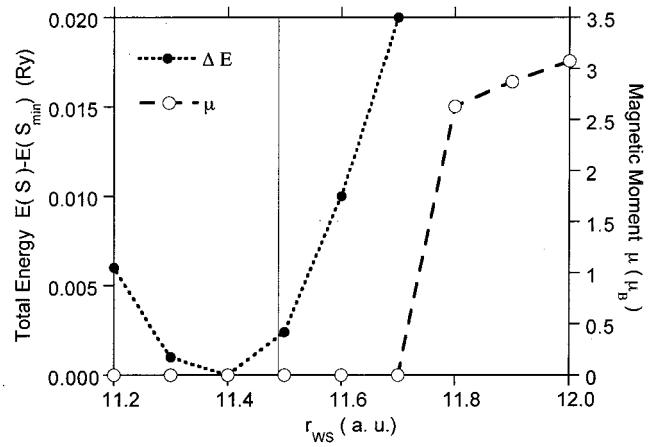

FIG. 4. Calculated magnetic moment and the total energy as a function of the Wigner-Seitz radius r_{WS} for Fe_2TiSn. The verticle line indicates the experimental value of r_{WS}.

T data between 1.8 and 300 K that exhibit typical semimetallic behavior above 50 K, but semiconductorlike behavior below 50 K. However, $\rho(T)$ does not display activated behavior; i.e., $\rho(T)$ does not vary as $e^{(\Delta E/k_BT)}$. The metallic behavior observed far below the Curie temperature suggests that the semiconducting behavior of $\rho(T)$ is closely related to the paramagnetic state of Fe_2TiSn. We conjecture that the lattice disorder complicates the metal-insulator transition, which is expected from the calculations of the bands near the Fermi level.

The LMTO valence-band calculations are compared to the XPS spectra in Fig. 3. The partial densities of states were convoluted by Lorentzians with a 0.4 eV half-width and multiplied by the corresponding cross sections taken from Ref. 7. The XPS valence band is extracted by means of a Tougaard algorithm.[8] The agreement between the theory, which predicts a nonmagnetic ground state for the Fe_2TiSn alloy, and the experimental data obtained for a sample at room temperature in the paramagnetic state, is excellent. However, a standard resolution of only 0.4 eV of the measured valence band XPS spectra makes it impossible to directly probe the gap at the Fermi level, in spite of the fact that the measured spectra are quantitatively similar to the convoluted DOS curves. It is interesting to note that a similar feature in the electronic structure and a semiconductorlike resistance anomaly have been observed in Fe_2VAl.[9–13] The compound Fe_2VAl has attracted a great deal of interest because the behavior of its specific heat is reminiscent of a heavy fermion material.[14] The compounds Fe_2VAl and Fe_2TiSn are similar in other respects; both appear to be in a marginally magnetic state and the electrical transport properties of both compounds resemble that of the narrow-gap semiconductor FeSi, which has been classified by Fisk *et al.*[15] as a unique *d*-electron system that belongs to the family of Kondo insulators. An example of a Kondo insulator that has been thoroughly studied is the compound CeNiSn,[16] which has a V-shaped pseudogap and a finite number of carriers at the Fermi level. However, recent measurements of the magnetic field dependence of the specific heat[17] indicate that the anomalous increase of the specific heat at low temperature in Fe_2VAl may be due to a sample-dependent Schottky anomaly originating from magnetic clusters associated with the Fe defects, suggesting conventional, rather than heavy fermion, behavior.

Shown in Fig. 5 are C/T vs T data below 30 K for Fe_2TiSn. The upturn in C/T at low temperature rises to $90\,\mathrm{mJ\,mol^{-1}\,K^{-2}}$, a value that is five times larger than that reported for Fe_2VAl.[17] We have fitted the data between 10 and 25 K to the expression $C(T)=\gamma T+\beta T^3+\delta T^5$, where the three terms represents the electronic, harmonic phonon and anharmonic phonon contributions, respectively. From this fit we obtained the values $\gamma=12\,\mathrm{mJ\,mol^{-1}K^{-2}}$, $\beta=0.11\,\mathrm{mJ\,mol^{-1}\,K^{-4}}$, and $\delta\cong 0$. The coefficient β of the low-temperature lattice contribution corresponds to a Debye temperature $\theta_D=260$ K, significantly lower than the value of 415 K inferred from the Debye-Waller factors measured at room temperature. A possible interpretation of the broad maximum in the specific heat at ~ 1.1 K is that it is a Schottky anomaly due to magnetic excitations within a two-level system with an energy level separation of k_BT_0.The relation $C(T)=\gamma T+\beta T^3+\delta T^5+\zeta[(T_0/T)^2$

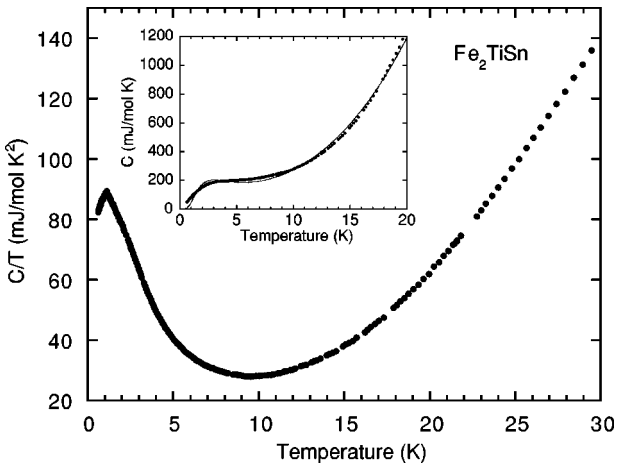

FIG. 5. Specific heat C divided by temperature T, C/T, vs T for Fe_2TiSn. The curve in the inset is a fit of the function described in the text to the $C(T)$ data.

$\times \exp T_0/T/(1+\exp T_0/T)^2]$, where the last term represents the Shottky contribution, has been fitted to that data as shown in the inset of Fig. 5 (solid curve). Using γ, β, and δ obtained above from the fit to the $C(T)$ data between 10 and 25 K, the parameters extracted from the fit that includes the Schottky contribution are $\zeta = 390\,\mathrm{mJ\,mol^{-1}\,K^{-1}}$ and $T_0 = 6.5$ K. The constant $\zeta = nR$, where n is the molar concentration of magnetic ions and R is the universal gas constant, has a value that is close to the value $\zeta = 208\,\mathrm{mJ\,mol^{-1}\,K^{-1}}$ expected for the concentration of Ti sites occupied by Fe ($n = 1/40$). While the low-temperature peak in the specific heat of Fe_2TiSn can be attributed to a Schottky anomaly, the mass enhancement evident in the C/T upturn is still indicative of heavy-fermion-like behavior. The effective mass corresponding to the value of γ determined from the fit is ~ 40 times the free-electron mass. Fe_2TiSn is an excellent example of a Heusler-type alloy, in which the local environment profoundly influences the magnetic and electrical transport properties.

One of us (A.Ś.) is grateful for the hospitality of the Institute for Pure and Applied Physical Sciences at UCSD and would like to express his appreciation to the Fulbright Foundation for support during his visit. The research of UCSD was supported by the U.S. Department of Energy under Grant No. DE FG03-86ER-45230. One of us (A.J.) thanks KBN for financial support (Project No. 2PB03B118.14), while another one of us (C.S.) thanks the Spanish MEC for financial support.

*On leave from Institute of Physics, University of Silesia, 40-007 Katowice, Poland.

[1] P.J. Webster and K.R.A. Ziebeck, in *Magnetic Properties of Metals*, edited by H. R. J. Wijn, Landolt-Börnstein New Series 1, Group III, Vol. 19, Pt. c, p. 75 (Springer, Berlin, 1988).

[2] Y. Fujita, K. Endo, M. Terada, and R. Kimura, J. Phys. Chem. Solids **33**, 1443 (1972); A. Szytuła, Z. Tomkowicz, and M. Turowski, Acta Phys. Pol. A **44**, 147 (1973).

[3] O.K. Andersen, and O. Jepsen, Phys. Rev. Lett. **53**, 2572 (1984); O.K. Andersen, O. Jepsen, and M. Sob, in *Electronic Structure and Its Applications*, edited by M. Yussouff (Springer, Berlin, 1987), p. 2.

[4] R.A. Young, and F. Izumi, in *The Rietveld Method*, edited by R. A. Young (Oxford University Press, Oxford, 1993), pp. 1 and 236.

[5] K. Lousdale, in *International Tables for X-ray Crystallography*, edited by K. Lousdale, C. H. MacGillavry, and G.D. Rieck (The Kynoch Press, Birmingham, 1962), Vol. III, p. 232.

[6] K. Kuriyama and F. Nakamura, Phys. Rev. B **36**, 4439 (1987).

[7] J.J. Yeh and I. Lindau, At. Data Nucl. Data Tables **32**, 1 (1985).

[8] S. Tougaard and P. Sigmund, Phys. Rev. B **25**, 4452 (1982).

[9] D.J. Singh and I.I. Mazin, Phys. Rev. B **57**, 14 352 (1998).

[10] R. Weht and W.E. Pickett, Phys. Rev. B **58**, 6855 (1998).

[11] C.S. Lue and J.H. Ross, Jr., Phys. Rev. B **58**, 9763 (1998).

[12] G.Y. Guo, G.A. Botton, and Y. Nishino, J. Phys.: Condens. Matter **10**, L119 (1998).

[13] A. Matsushita and Y. Yamada, J. Magn. Magn. Mater. **196-97**, 669 (1999).

[14] Y. Nishino, M. Kato, S. Asano, K. Soda, M. Hayasaki, and U. Mizutani, Phys. Rev. Lett. **79**, 1909 (1997).

[15] Z. Fisk, J.L. Sarrao, S.L. Cooper, P. Nyhus, G.S. Boebinger, A. Passner, and P.C. Canfield, Physica B **223-224**, 409 (1996); Z. Schlesinger, Z. Fisk, H.T. Zhang, M.B. Maple, J.F. DiTusa, and G. Aeppli, Phys. Rev. Lett. **71**, 1748 (1993); S. Paschen, E. Felder, M.A. Chernikov, L. Degiorgi, H. Schwer, H.R. Ott, D.P. Yong, J.L. Sarrao, and Z. Fisk, Phys. Rev. B **56**, 12 916 (1997).

[16] T. Takabatake, F. Teshima, H. Fujii, N. Nishigori, T. Suzuki, T. Fujita, Y. Yamaguchi, J. Sakurai, and D. Jaccard, Phys. Rev. B **41**, 9607 (1990).

[17] C.S. Lue, J.H. Ross, Jr., C.F. Chang, and H.D. Yang, Phys. Rev. B **60**, R13 941 (1999).